

OPEN ACCESS

Localized Stress Effects on the Single Event Effects Sensitivity of Microelectronics

To cite this article: Sergei P. Stepanoff *et al* 2024 *ECS J. Solid State Sci. Technol.* **13** 065004

View the [article online](#) for updates and enhancements.

You may also like

- [CHARGING OF DUST GRAINS IN ASTROPHYSICAL ENVIRONMENTS BY SECONDARY ELECTRON EMISSIONS](#)
M. M. Abbas, D. Tankosic, A. C. LeClair et al.
- [Effect of asymmetric secondary emission in bounded low-collisional \$E \times B\$ plasma on sheath and plasma properties](#)
Hongyue Wang, Michael D Campanell, Igor D Kaganovich et al.
- [A Comparative Analysis of the Solar Ultraviolet Spectral Irradiance Measured from Earth and Mars: Toward a General Empirical Model for the Study of Planetary Aeronomy](#)
Zhen Xu and Jianqi Qin

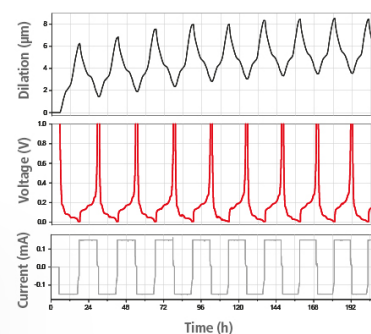
Watch Your Electrodes Breathe!

Measure the Electrode Expansion in the Nanometer Range with the ECD-4-nano.

- ✓ Battery Test Cell for Dilatometric Analysis (Expansion of Electrodes)
- ✓ Capacitive Displacement Sensor (Range 250 μm , Resolution ≤ 5 nm)
- ✓ Detect Thickness Changes of the Individual Half Cell or the Full Cell
- ✓ Additional Gas Pressure (0 to 3 bar) and Temperature Sensor (-20 to 80° C)



EL-CELL[®]
electrochemical test equipment



See Sample Test Results:



Scan me!

Download the Data Sheet (PDF):



Scan me!

Or contact us directly:

+49 40 79012-734

sales@el-cell.com

www.el-cell.com



Localized Stress Effects on the Single Event Effects Sensitivity of Microelectronics

Sergei P. Stepanoff,^{1,2} Ani Khachatryan,^{3,z} Aman Haque,^{4,z} Fan Ren,^{5,*} Stephen Pearton,^{6,*} and Douglas E. Wolfe^{1,2,7,8,z}

¹Materials Science and Engineering Department, The Pennsylvania State University, University Park, Pennsylvania 16802, United States of America

²Applied Research Laboratory, The Pennsylvania State University, University Park, Pennsylvania 16802, United States of America

³United States Naval Research Laboratory, Washington, DC 20375, United States of America

⁴Mechanical Engineering, The Pennsylvania State University, University Park, Pennsylvania 16802, United States of America

⁵Chemical Engineering, University of Florida, Gainesville, Florida 32611, United States of America

⁶Material Science and Engineering, University of Florida, Gainesville, Florida 32611, United States of America

⁷Engineering Science and Mechanics Department, The Pennsylvania State University, University Park, Pennsylvania 16802, United States of America

⁸Ken and Mary Alice Lindquist Nuclear Engineering Department, The Pennsylvania State University, University Park, Pennsylvania 16802, United States of America

Understanding the single event effects (SEE) sensitivity of microelectronic devices and circuits is essential for long-term mission success in ionizing radiation environments. SEEs occur when a single ionizing particle strikes a device with enough energy to cause anomalous malfunction or even a catastrophic failure event. It is conventionally viewed as an electrical phenomenon, whereas this study investigates the possible role of multi-physics. Specifically, we show that localized mechanical stress in electronic devices significantly impacts the degree of SEE sensitivity. We present a technique that indirectly maps both electrical and mechanical field localization to spatially map SEE sensitivity without any need for radiation test sources. It is demonstrated on the operational amplifier LM124 under both pristine and stressed conditions. To validate our hypothesis, our experimental results are compared with those obtained from the well-established pulsed laser SEE technique. Excellent agreement between these results supports our hypothesis that SEE susceptibility may have fundamental roots in both electrical and mechanical fields. Therefore, the ability to map the localizations in these fields may indirectly map the SEE sensitivity of large area electronics, which is very expensive in time and resources.

© 2024 The Author(s). Published on behalf of The Electrochemical Society by IOP Publishing Limited. This is an open access article distributed under the terms of the Creative Commons Attribution 4.0 License (CC BY, <http://creativecommons.org/licenses/by/4.0/>), which permits unrestricted reuse of the work in any medium, provided the original work is properly cited. [DOI: 10.1149/2162-8777/ad522a]



Manuscript submitted December 24, 2023; revised manuscript received June 5, 2024. Published June 7, 2024.

Single event effects (SEE) are a class of ionizing radiation effects caused by a single, energetic particle that can result in anomalous device behavior and circuit response. SEEs normally appear as spurious electrical transients in integrated or analog circuits, and the transients can confuse the logical operation, such as flipping memory cells, to cause soft errors.¹ The fundamental challenge lies in quantifying charge density, diffusion, drifting, and recombination dynamics following ionization. Such effects can be particularly problematic in mission-critical applications in space, where electronic heavy ions and protons pose a threat.² SEE may manifest in many forms, such as Single Event Upset (SEU), Single Event Latch-up (SEL), and Single Event Burnout (SEB). SEUs are single bit upsets that change memory or logic functions and are caused by the disruption of the device's charge state, while SEL is a more severe form of SEU that can result in permanent damage to the device. SEB occurs in power devices, such as transistors, and results in the destruction of the device due to high current or voltage.^{3,4}

Identifying the most sensitive regions in electronic systems is necessary for the efficient enhancement in the radiation hardness of an electrical device, but it can be a time-consuming process, particularly for large and complex systems.⁵⁻⁸ The most reliable technique for SEE involves exposing devices to radiation sources, such as heavy ions⁹ or high-energy neutrons¹⁰ and monitoring the response of the circuit. This form of radiation effects testing occurs in a controlled environment, where the ionizing particles or waves are only allowed to interact with the device under test (DUT), while shielding may be used to collimate the beam toward the region of

interest if a broad beam is utilized or an accelerated beam of particles may be focused on the regions of interest.³ During these tests, the device performance is monitored to indicate the SEE sensitive regions. While radiation tests are the most direct and accurate representation of the SEE vulnerability, they are extremely complex to set up because of the pre-requisite knowledge of the three-dimensional device structure, circuits, and material-dependent charge transport physics to name a few.^{4,6} Scarcity of proton or heavy ion sources make such tests both time and resource intensive, which can be alleviated with prior simulation of the device or circuit. Other complementary methods use pulsed-laser or X-ray based radiation that are almost exclusively focused to point-like beams, then scanned across a device to identify the regions that generate the highest number of upsets.¹¹⁻¹³ Another approach is to simulate fault injection to observe how a device responds when a certain, known component is corrupted.^{14,15} These techniques significantly speed up the characterization process. However, that advantage is continually outpaced by the increase in size and complexity of modern electronics.⁵ There is a strong need for faster and accurate techniques that spatially map the most vulnerable regions (MVR) with minimum pre-requisite knowledge of the DUT and without specialized resources. This provides the motivation for this study.

Figure 1 shows the core components of this study. It is based on a multi-physics driven hypothesis that highly localized and large magnitude mechanical strain (or stress) significantly enhances the charge generation and transport. Or in other words, our technique searches for the overlapping of electrically and mechanically sensitive areas to achieve higher accuracy. Figure 1a shows the existing model for SEE, an ionizing particle hitting the drain end of the gate of a transistor, where the localized electrical field is the highest. The contribution of this study is to account for the

*Electrochemical Society Fellow.

^zE-mail: mah37@psu.edu; ani.khachatryan@nrl.navy.mil; dew125@psu.edu

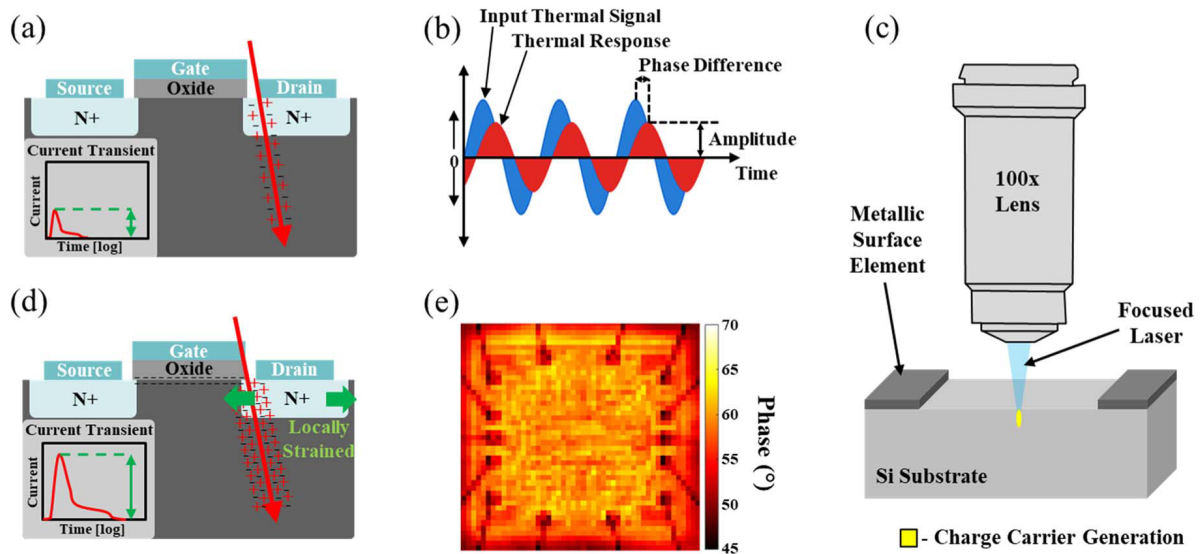


Figure 1. Schematics showing (a) and (d) the effect of stress on the level of charge generation and deposition into a device, (b) and (e) how lock-in thermography is used to generate maps of stress and inhomogeneity, and (c) pulsed-laser single event transient technique.

mechanical stress localization (Fig. 1d). Such stress/strain localization is ubiquitous in electronic devices; anywhere there are sharp changes in device geometry and materials. Furthermore, stress and strain can also affect the reliability of electronic systems over time. The accumulation of stress and strain can cause devices to fail prematurely or develop defects that can affect their performance. This can be particularly problematic in high radiation environments, where devices are already under significant stress. It is important to note that we are not investigating the global or average strain, which could be negligible. Rather, we argue that very high values of localized strain reflect higher internal energy and thus greater susceptibility to a single energetic particle. Our multi-physics approach allows us to develop an experimental philosophy where the objective is to spatially map the relative SEE sensitivity over the entire system instead of the current practice of absolute measurement of single event transients. This results in an indirect, black box type but multi-physics driven technique, where the notable advantage is that we can capture such localization over large area electronics with a unique thermal phase lag microscopy that utilizes focal plane array imaging instead of raster scan. This is described below.

We exploit thermal phase lag microscopy to identify the mechanical stress/strain localizations. Here, a thermal wave is sent to the surface of the system as we examine its reflections from the various materials layers and geometry. The stress localizations are detected by the loss of the energy reflected by the phase lag between the input and output waveforms. This is shown in Fig. 1b. The accuracy of the technique depends on optimal modulation of the input frequency. This can be achieved by frequency filtering through software or hardware based lock-in.¹⁶ Instead of rastering, we use a focal plane array infrared microscope to capture the stress localization over a large area in a single snap (Fig. 1e). This significantly accelerates the characterization process as we have demonstrated previously.^{17,18} The spatial resolution is dictated by infrared microscope specifications. For example, 25×25 pixel resolution of a focal plane array does not “resolve” but accurately “discerns” the sensitive areas (similar to detecting a sub-micron feature with white light microscopy).

The objective of this study is to validate our core hypothesis that localized large magnitude mechanical strain (or stress) significantly enhances the charge generation and transport. Accordingly, we prepare specimens of the same operational amplifier with two different conditions, pristine and electrically stressed. The electrical stressing process involves DC biasing of a certain component of the op-amp at higher than the rated voltage and for prolonged period of

time. This results in amplifying the mechanical stress localizations that exist in the pristine condition. The specimens are studied under both the proposed multi-physics and pulsed-laser Single Event Transient (PL-SET) testing for validation. PL-SET is a state-of-the-art technique used to identify SEE sensitive regions. Here, pulsed lasers are used to create high-energy carriers in the device, simulating the effect of ionizing radiation. These charge carriers can cause transient response in device behavior, which can be observed and analyzed (Khachatryan et al., 2016). Both temporal and spatial information can be extracted by scanning the laser across the device and monitoring the characteristics of the resulting single event transients (SETs). The technique is well-established in the literature and shows good agreement with heavy ion testing results.^{7,19,20} Further details are given in the next sections.

Materials and Methods

In order to test the effect of localized stress on device sensitivity to ionizing radiation, two Texas Instrument LM124 operational amplifiers were tested as a function of stress. Both LM124s were decapsulated, and one was examined in the pristine, as-received condition while the other was stressed before examination. The focus of the study was on transistor Q1 (or “QR1”), shown in Fig. 2, which has been identified in the literature as the most sensitive transistor on the LM124.^{12,18,20} In order to stress the transistor, probe needles were contacted on the leads of QR1 as shown in Fig. 2a, where the probe on the right was biased at +30 V DC and the left probe was held at ground for a period of 24 h. These voltages exceed the manufacturer’s limits the entire LM124, imparting residual mechanical stress into the region of transistor QR1.

Pulsed-laser single event transient testing was utilized to examine the effect of the stress difference on the sensitivity of the transistor as it is a well validated technique with the necessary resolution and capability to quantify the deposition of charge carriers into the circuitry.²¹ The technique offers a powerful means of validating the SEE sensitive regions identified through our proposed thermal phase lag microscopy based method. For the pulsed-laser technique, a focused and pulsed laser beam is used to generate localized, transient events within the microelectronic device, mimicking the effects of ionizing radiation.⁷ Figure 3 shows the schematic setup of the pulsed-laser system. The devices were tested topside with 590 nm laser light at a repetition rate of 1 kHz and a pulse width of 250 fs. At this wavelength, the laser photon energy exceeds the bandgap of silicon, inducing charge generation in the semiconducting material

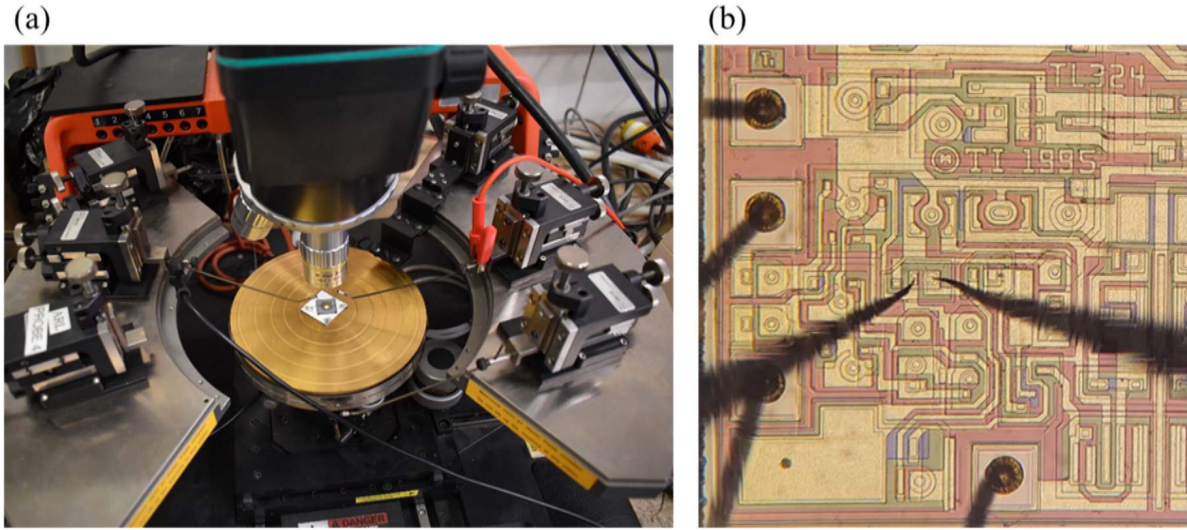


Figure 2. (a) Electrical stressing apparatus for the LM124 with a (b) micrograph showing the positioning of the probes, where the probe on the left was held at GND and the probe on the right was held at +30 V DC for 24 h.

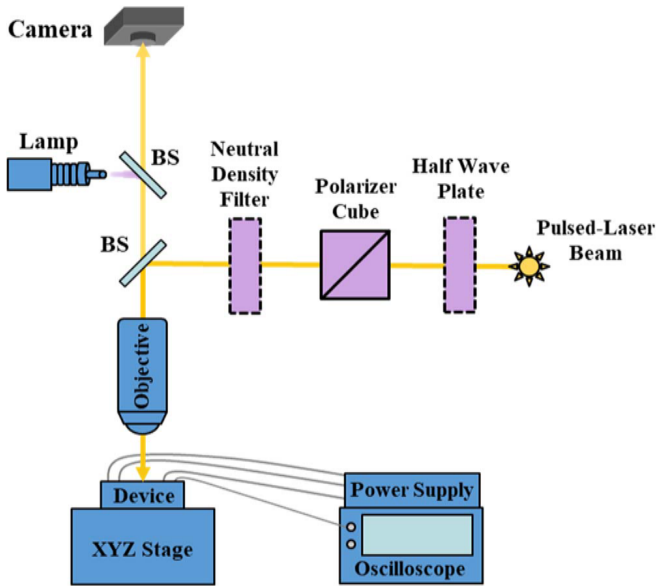


Figure 3. Schematic of pulsed-laser setup for single event transient measurement on the operational amplifier LM124.

within the DUT via a single-photon absorption process. A 100x objective was used to focus the laser beam to full width at half max of 0.8 μm .

The LM124 was configured as a voltage follower for the pulsed-laser experiments as shown in Fig. 4c. Transistor QR1, which is shown in Fig. 4b, was the focus of this study. During pulsed-laser measurements on QR1, the LM124 was powered, and the V_{out} readings were recorded with a Tektronix 16 GHz, 50 GS/s digital phosphor oscilloscope. During laser testing $V_{\text{in}} = 5 \text{ V}$ $V_{\text{dd}} = 15 \text{ V}$. An average of 20 SETs were recorded as a function of position during the experiments on the LM124. In order to calculate the amount of collected charge the integral of the SETs was taken and divided by oscilloscope channel impedance, which was 1 MOhm.

Thermal phase lag microscopy experiments were conducted using an Optris PI 640 IR camera with a thermal sensitivity of 75 mK over the spectral range of 8–14 μm . The setup comprises three components, including an infrared (IR) camera, a thermal excitation source, and a signal processing tool. An IR microscopic lens with a focal distance of 41.5 mm and a resolution of 28 μm was

used. All measurements were acquired at a frame rate of 32 Hz, which is the standard framerate of the PI 640 camera. Thermal lamps were used to probe the LM124 with heat waves that were pulsed using a two-channel 5 V relay module and a programmable Arduino board.

Lock-in thermography (LIT) was used to identify the regions of localized stress and strain that provide a mechanical means of identifying the most vulnerable regions of the LM124. The technique produces an emissivity corrected phase map by injecting thermal waves at a constant lock-in frequency with the thermal lamps, while the reemitted thermal signal is measured with the thermal camera. The temperature data of each thermal camera pixel with respect to time was multiplied by two sinusoidal orthogonal weighting factors— $\sin(t)$ and $-\cos(t)$ —each with a frequency that matches the lock-in frequency. The results were summed for each pixel, to produce two values associated with each pixel bin, including S^{0° , the in-phase component of the reemitted signal, and S^{-90° , the out-of-phase component of the reemitted signal (Wang et al., 2018). Using both S^{0° and S^{-90° signals, the phase (φ) value for each pixel, which represents the degree of lag between the reemitted thermal signal vs a reference signal, can be calculated using Eq. 1. The regions that exhibit the highest difference in phase contrast values correspond to the regions with the highest thermal stopping power due to manufactured strain based on the underlying structure of the device.

$$\varphi = \tan^{-1} \left(\frac{S^{-90^\circ}}{S^{0^\circ}} \right) \quad [1]$$

Electrically relevant regions on the LM124 are identified by powering the LM124 and observing the regions that exhibit the highest temperature change as a result of Joule heating. By considering both the mechanical and electrical metrics for MVR prediction, regions sensitive to SEE are identified.

Results

Current transients with positive and negative peaks were observed from the pulsed laser data for both tested boards. This indicates that delocalized electrons initially flowed in one direction immediately after the laser pulse, then reversed flow during the subsequent energetic equilibration. Figure 5a shows the average of 20 SETs from when laser beam is focused in the channel region of transistor QR1, which is shown in the subset of the figure with a visible laser spot. Figure 5b shows the charge collected, which is calculated from the total area under the curve

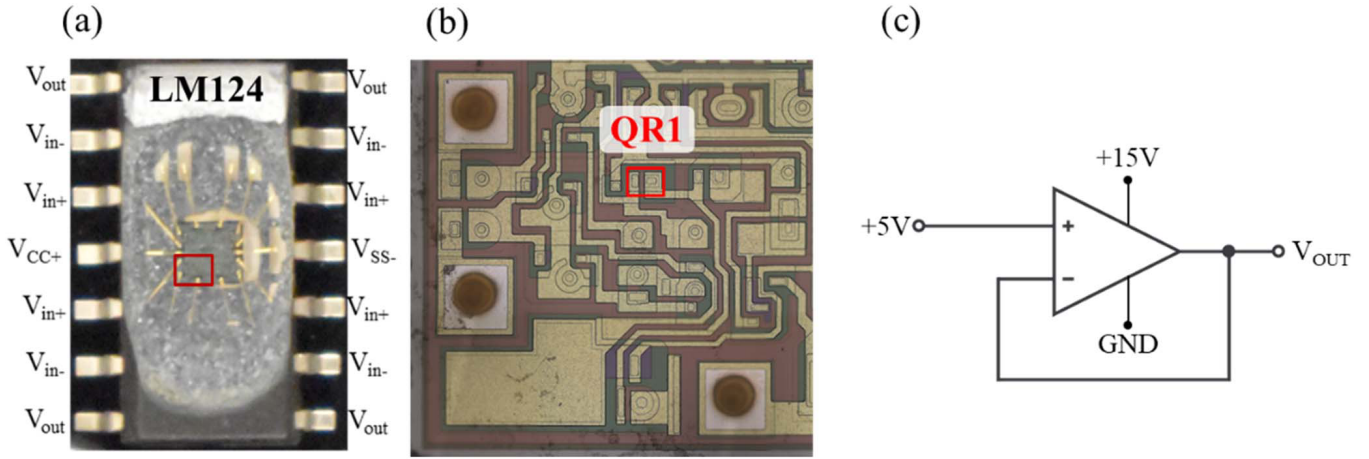


Figure 4. (a) Digital image of TI LM124 with labelled pin out, (b) optical micrograph of the quadrant of interest, and (c) configuration of the LM124 while under test for PL-SET characterization.

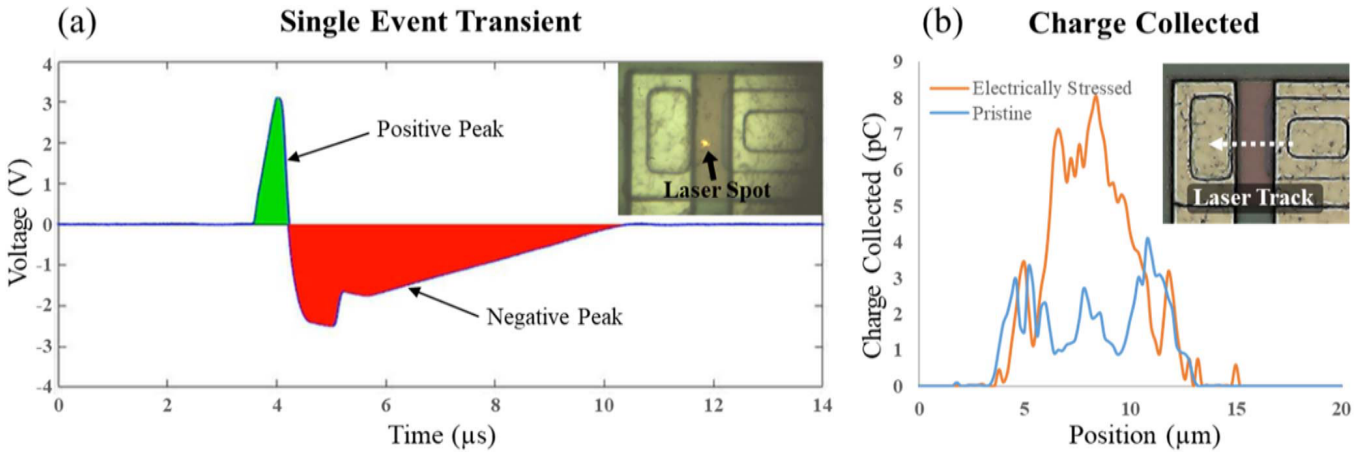


Figure 5. (a) Single event transients generated as a result of the 590 nm 30.1 pJ laser pulse interacting with the channel region in transistor QR1 on the LM124 and (b) the resulting charge collected of a line scan across the channel region.

of the SETs, as a function of position across the channel region of transistor QR1, and it is clear that the stressed sample produces more charge carriers, increasing the likelihood and severity of upsets.

Current transients were collected when laser was scanned across the channel of transistor QR1 and the area under the curve of the positive and negative peaks of the transients were quantified. The total charge collected in the circuit during the laser pulses can be directly calculated from the area of the positive and negative peaks in the current transient data. The larger the peaks and area under the curve, the more charge carriers deposited into the circuit, therefore producing a higher amount of potential damage or upsets through SEE. The 2D mapping results of transistor QR1 are shown in Fig. 6 and clearly show that the stressed DUT produced much larger SETs, an overall larger collected charge for the same position and laser energy. For these 2D maps median charge collected for the stressed device is 2.7 pC higher than for the pristine one. This provides strong supporting evidence for the hypothesis that higher localized stress results in higher sensitivity to radiation effects.

Lock-in thermography and thermoelectric analysis was also conducted on the LM124 as shown in Fig. 7. Together, these metrics were used to predictively map the overall radiation sensitivity of the LM124 using (1) thermal phase lag analysis to identify regions of high strain and (2) joule heating from device biasing to identify areas of electrical activity. These metrics were assembled into a composite score using Eq. 2, where φ is the phase value.

$$\text{Composite Score} = \text{Normalize} \left[\text{Abs} \left(\frac{\varphi - \varphi_{\text{avg}}}{\varphi_{\text{max}} - \varphi_{\text{min}}} \right) \left(\frac{T - T_{\text{min}}}{T_{\text{max}} - T_{\text{min}}} \right) \right] \quad [2]$$

For the analysis, the LM124 was sectioned to better visualize the composite data region by region. Of note, the resolution of the utilized thermography techniques is limited by the resolution of the imaging system, which is inherently diffraction limited by the wavelength of light used. Higher spatial resolution results can be achieved with a NIR wavelength as opposed to the 8–14 μm spectral range used for imaging. A higher value for the composite score indicates higher sensitivity to ionizing radiation, by accounting for extreme phase values that indicate positive or negative strain as well as large temperature change due to biasing. Of the mechanical and electrical metrics that make up the score, one is not necessarily more significant than the other in terms of their impact on the degree of vulnerability to ionizing radiation because they are both conditions necessary to cause SEEs.

Excluding regions that are known to be irrelevant to the effects of ionizing radiation, such as the wire bonded pads that give an anomalously high composite score, the regions that give the highest composite scores on the LM124 quadrant, and therefore the highest expected sensitivity, overlap with transistor QR1, which has been shown in the literature to be the most sensitive to ionizing radiation on the LM124. It is necessary to note that regions along the edge of

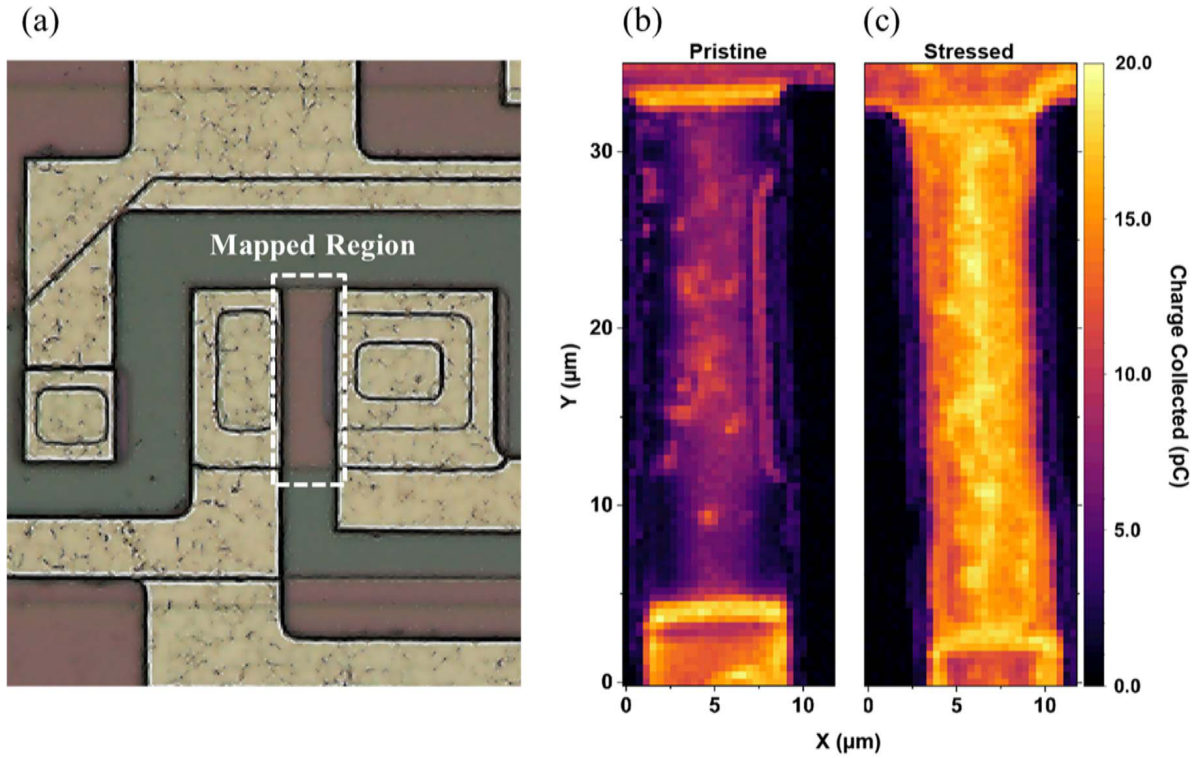


Figure 6. (a) Optical micrograph of transistor QR1 of the LM124 operational amplifier with 2D collected charge maps of the channel region of the (b) pristine and (c) locally stressed QR1 transistors.

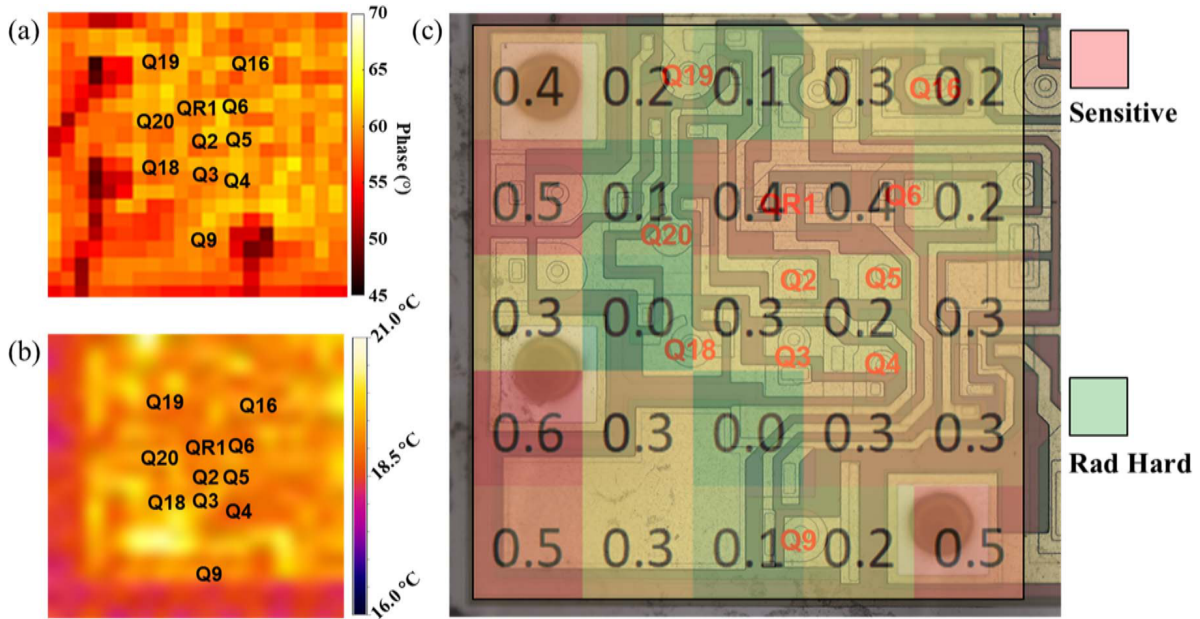


Figure 7. (a) Phase analysis of LM124 using the lock-in thermography technique, (b) thermal micrograph of a powered LM124, and (c) a visible light optical micrograph of the LM124 with labelled transistors overlaid with a composite metric for mechanical and electrical hotspots.

the LM124 may also produce a higher composite score due to overlap and interaction with surrounding insulation material that remained present after decapsulation of the LM124.

Conclusions

We proposed a new experimental technique for fast and accurate spatial mapping of the SEE sensitive regions in large area electronics. The technique does not need radiation/pulsed laser/X-rays since it infers SEE sensitivity from electrical and mechanical field

localizations (“hotspots”) with lower threshold energy. The technique is very fast because (1) no “reverse engineering” or prior knowledge of device design and circuit layout is necessary and (2) the whole DUT is imaged at once. It can be orders of magnitude faster than ion beam and pulsed-laser techniques. For example, our technique can process $10 \times 10 \text{ mm}^2$ area in $<1 \text{ h}$. In comparison, pulsed laser technique may take 50–75 h to raster at $5\text{--}20\times$ magnification. Ion micro-beam may take a few weeks to probe pre-selected regions and complete chip testing, which is not feasible due to time. We suggest that our technique can strongly impact the

efficiency of ion beam based radiation testing by providing quick screening of SEE sensitivity in complex systems. The outcome can lead to optimization of the ion beam and scanning parameters for radiation-based testing by screening without the need for detailed knowledge of device structure.

The contribution of this study is experimental evidence validating the hypothesis that mechanical stress localizations can be useful in reducing complexity of SEE testing. Our experimental results show that localized stress has a significant impact on the sensitivity of microelectronics to single event effects (SEE), producing larger single event transients than that of pristine devices. This is an important first step towards a rigorous validation protocol needed for our multi-physics driven black box technique. We envision this technique to be adopted as a quick scouting of SEE sensitive regions in large area electronics (such as System on Chips) and provide critical information to optimize ion beam based testing.

Acknowledgments

The work at PSU and UF was performed as part of Interaction of Ionizing Radiation with Matter University Research Alliance (IIRM-URA), sponsored by the Department of the Defense, Defense Threat Reduction Agency under Award No. HDTRA1-20-2-0002. The content of the information does not necessarily reflect the position or the policy of the federal government, and no official endorsement should be inferred. A.H. also acknowledges support from the U.S. National Science Foundation (ECCS No. 2015795).

ORCID

Aman Haque  <https://orcid.org/0000-0001-6535-5484>

Stephen Pearton  <https://orcid.org/0000-0001-6498-1256>

References

1. S. J. Pearton, A. Haque, A. Khachatryan, A. Ildefonso, L. Chernyak, and F. Ren, "Review—Opportunities in Single Event Effects in Radiation-Exposed SiC and GaN Power Electronics." *ECS J. Solid State Sci. Technol.*, **10**, 075004 (2021).
2. D. M. Fleetwood and R. D. Schrimpf, *Radiation Effects and Soft Errors in Integrated Circuits and Electronic Devices* (World Scientific, Singapore) (2004).
3. K. Tapero, *Radiation Effects on the Integrated Circuits and Systems for Space Applications*, ed. R. Velazco, D. McMorrow, and J. Estela (Springer, Cham, Switzerland) (2019).
4. G. F. Knoll, *Radiation Detection and Measurement*, ed. J. Welter and D. Matteson (Wiley, Hoboken, NJ) (2010).
5. D. M. Fleetwood, "Radiation Effects in a Post-Moore World." *IEEE Trans. Nucl. Sci.*, **68**, 509 (2021).
6. V. Ferlet-Cavrois, L. W. Massengill, and P. Gouker, "Single Event Transients in Digital CMOS—A Review." *IEEE Trans. Nucl. Sci.*, **60**, 1767 (2013).
7. J. M. Hales et al., "New Approach for Pulsed-Laser Testing That Mimics Heavy-Ion Charge Deposition Profiles." *IEEE Trans. Nucl. Sci.*, **67**, 81 (2020).
8. J. R. Schwank, M. R. Shaneyfelt, and P. E. Dodd, "Radiation Hardness Assurance Testing of Microelectronic Devices and Integrated Circuits: Radiation Environments, Physical Mechanisms, and Foundations for Hardness Assurance." *IEEE Trans. Nucl. Sci.*, **60**, 2074 (2013).
9. W. Yang, X. Du, C. He, S. Shi, L. Cai, N. Hui, G. Guo, and C. Huang, "Microbeam Heavy-Ion Single-Event Effect on Xilinx 28-nm System on Chip." *IEEE Trans. Nucl. Sci.*, **65**, 545 (2018).
10. J. C. Fabero, H. Mecha, F. J. Franco, J. A. Clemente, G. Korkian, S. Rey, B. Cheymol, M. Baylac, G. Hubert, and R. Velazco, "Single Event Upsets Under 14-MeV Neutrons in a 28-nm SRAM-Based FPGA in Static Mode." *IEEE Trans. Nucl. Sci.*, **67**, 1461 (2020).
11. D. Bisello, A. Candelori, N. Dzysiuik, J. Esposito, P. Mastinu, S. Mattiazzo, G. Prete, L. Silvestrin, and J. Wyss, "Neutron production targets for a new Single Event Effects facility at the 70 MeV Cyclotron of LNL-INFN." *Phys. Proc.*, **26**, 284 (2012).
12. S. P. Buchner, F. Miller, V. Pouget, and D. P. McMorrow, "Pulsed-Laser Testing for Single-Event Effects Investigations." *IEEE Trans. Nucl. Sci.*, **60**, 1852 (2013).
13. C. Gu, R. Chen, G. Belev, S. Shi, H. Tian, I. Nofal, and L. Chen, "Application of Two Photon-Absorption Pulsed Laser for Single-Event-Effects Sensitivity Mapping Technology." *Materials (Basel, Switzerland)*, **12**, 1 (2019).
14. S. Duzellier, J. P. David, C. Inguibert, T. Nuns, G. Hubert, and L. Artola, "Radiation Testing of Electronics Systems: How Can Simulation Tools Help in the Definition and Optimization of Test Plans in Labs?" *Aerospace Lab*, **12**, 1 (2016).
15. A. M. Keller and M. J. Wirthlin, "The Impact of Terrestrial Radiation on FPGAs in Data Centers." *ACM Trans. Reconfigurable Technol. Syst.*, **15**, 12 (2021).
16. O. Breitenstein, W. Warta, and M. C. Schubert, *Lock-in Thermography: Basics and Use for Evaluating Electronic Devices and Materials*, ed. K. Chun, K. Itoh, T. H. Lee, R. Micheloni, T. Sakurai, W. M. C. Sansen, and D. Schmitt-Landsiedel (Springer, Cham, Switzerland) (2018).
17. S. P. Stepanoff, A. Haque, F. Ren, S. Pearton, and D. E. Wolfe, "Rapid detection of radiation susceptible regions in electronics." *J. Vac. Sci. Technol. B*, **41**, 044005 (2023).
18. S. P. Stepanoff, M. A. J. Rasel, A. Haque, D. E. Wolfe, F. Ren, and S. J. Pearton, "Heuristic Detection of the Most Vulnerable Regions in Electronic Devices for Radiation Survivability." *ECS J. Solid State Sci. Technol.*, **11**, 085008 (2022).
19. J. M. Hales, A. Ildefonso, S. P. Buchner, A. Khachatryan, G. Allen, and D. McMorrow, "Quantitative Prediction of Ion-Induced Single-Event Transients in an Operational Amplifier Using a Quasi-Bessel Beam Pulsed-Laser Approach." *IEEE Trans. Nucl. Sci.*, **70**, 354 (2023).
20. R. L. Pease, A. L. Sternberg, Y. Boulghassoul, L. W. Massengill, S. Buchner, D. McMorrow, D. S. Walsh, G. L. Hash, S. D. LaLumondiere, and S. C. Moss, "Comparison of SETs in bipolar linear circuits generated with an ion microbeam, laser light, and circuit simulation." *IEEE Trans. Nucl. Sci.*, **49**, 3163 (2002).
21. A. Khachatryan, N. J.-H. Roche, D. McMorrow, J. H. Warner, S. P. Buchner, and J. S. Melinger, "A Dosimetry Methodology for Two-Photon Absorption Induced Single-Event Effects Measurements." *IEEE Trans. Nucl. Sci.*, **61**, 3416 (2014).